

High Bandwidth Stagnation Temperature Measurements in a Mach 6 Gun Tunnel Flow

D. R. Buttsworth

Faculty of Engineering and Surveying

University of Southern Queensland

Toowoomba, Australia 4350

buttswod@usq.edu.au

T. V. Jones

Department of Engineering Science

Oxford University

Oxford, England OX1 3PJ

terry.jones@eng.ox.ac.uk

Abstract

Temperature is an important parameter in most high speed flow experiments, but it is sometimes a difficult parameter to measure, particularly in short-duration facilities. Stagnation temperature measurements have been obtained using transient thin film heat flux probes in a Mach 6 carbon dioxide flow produced by the Oxford University Gun Tunnel. The probes were operated over a range of surface temperatures so that the flow stagnation temperature could be identified independently of the convective heat transfer coefficient of the probes. The time-averaged measurements indicate a significant drop in stagnation temperature with time and this implies that significant cooling of the test gas occurred within the barrel during the compression process and/or during the flow discharge process. During the last 12ms of flow, the time-averaged stagnation temperature indicated by the probe was $610 \pm 10\text{K}$ for the present operating conditions. During the same 12ms flow period, the probe measurements also indicate stagnation temperature fluctuations of about 2.3K (RMS) for frequencies between 1 and 25kHz. Based on pitot pressure fluctuation measurements at essentially the same location within the nozzle, it is concluded that the measured temperature fluctuations are primarily due to fluctuations in entropy. Entropy fluctuations within the Mach 6 flow probably arise because of the turbulent heat transfer to the barrel.

1 Introduction

Gun tunnel facilities use a free piston compression process to produce a high pressure gas reservoir at moderate temperatures (around 1000K). This gas reservoir can then be expanded with an appropriate nozzle contour to produce a short duration (less than one second) test flow for gasdynamics and aerodynamics experiments.

The Oxford University Gun Tunnel was originally designed and commissioned as a Bristol Siddeley facility and has been used in a variety of experiments including scramjet testing, quiescent [1] and coflowing [2] rocket plume studies, hypersonic mixing studies [3],[4] and aerodynamics experiments. Another active gun tunnel facility is the Imperial College Gun Tunnel which has recently been used in studies of hypersonic boundary layer development with pressure gradient effects [5]. To provide useful experimental data, it is important to accurately define the flow conditions produced by any wind tunnel facility. To this end, Mallinson et al. [6] used a number of different experimental techniques including pressure and transient heat flux measurements combined with calculations and computational predictions to quantify the time-averaged Mach 9 flow conditions produced by the Imperial College Gun Tunnel.

Stagnation temperature is an important parameter in most hypersonic flow experiments. In an attempt to identify the Imperial College Gun Tunnel flow stagnation temperature, Mallinson et al. [6] used thin

film gauges located close to the stagnation point of two different diameter hemisphere-cylinder probes. The intention of their experiments was to identify the stagnation temperature from measurements of transient heat flux combined with a convective heat transfer coefficient determined from computational predictions. While satisfactory values of time-averaged stagnation temperature appear to have been obtained with the small diameter probe, the larger diameter probe indicated inexplicably high stagnation temperatures.

Fluctuations within the free stream flow conditions produced by wind tunnels can have a significant effect on the results produced during the experiment. The level and distribution of free stream disturbances can be particularly significant in shear layer transition experiments. Without sufficient free stream disturbance data it may be difficult to apply the wind tunnel data to flight conditions, or adequately test theoretical predictions and simulations of the wind tunnel results. Significant free stream disturbance measurement have been obtained in conventional supersonic and hypersonic facilities typically using hot wire or pitot pressure devices, and low noise facilities have now been designed [7]. However, little data is available on free stream fluctuations within transient hypersonic facilities. Pressure fluctuations have been measured with a pitot probe in a free piston shock tunnel [8], but it appears the protective cavity ahead of the transducer induced an aerodynamic resonance at about 10kHz which is too close to the frequencies of interest. Fluctuations within a laminar boundary layer on a cone model in a shock tunnel flow have also been reported [9], but no attempt was made to relate the measurements to free stream disturbances. RMS fluctuations in stagnation point heat flux measurements in a shock tunnel flow have also been reported [10], but it was not possible to clearly identify probe-independent flow parameters from the measurements.

The present work describes the application of transient thin film heat flux gauges to the measurement of time-averaged and fluctuating stagnation temperatures in the Oxford University Gun Tunnel. It may have been possible to use other probe devices such as an aspirating probe [11] (for measurements at frequencies less than 20kHz), or thermocouple probes [12] (for measurements at frequencies less than 1kHz). However, stagnation temperature probes utilizing transient heat flux gauge technology are capable of producing high bandwidth data, typically to around 100kHz. Such probes have already been demonstrated in various configurations and flows [13],[14],[15],[16]. Furthermore, in situations with high transient loads and the possibility of particulate matter within the flow, stagnation temperature measurements can be obtained with these devices because they are relatively robust.

2 Gun Tunnel Facility

The Oxford University Gun Tunnel barrel has a length of 9m and an internal diameter of 96.3mm. Details on the Oxford University Gun Tunnel are provided by Cain [1]. The initial absolute filling pressures for the current experiments were: 7.70 ± 0.15 MPa of air in the driver, and 194 ± 3 kPa of carbon dioxide in the barrel. Carbon dioxide was used as the test gas because simulation of a Martian entry condition was required. The initial temperature of the carbon dioxide within the barrel was not measured directly, but it is expected to be 291 ± 2 K. This is because the ambient temperature of the gun tunnel and laboratory was quite close to 18°C throughout the experimental program, and the barrel filling process was slow and was completed at least 10 minutes prior to a run. The initial temperature of the air driver immediately prior to diaphragm rupture was also not directly measured, but in this case, the uncertainty in the actual temperature is somewhat larger because the rapid filling process occurred over a period of about 1 minute prior to the run and some heat was transferred to the driver gas from the filling line. However, precise information on the air driver temperature is not required for identification of the test gas temperature arising from the shock compression process within the barrel.

The gun tunnel was operated with a contoured nozzle that was designed to produce a Mach 7 flow with a nitrogen test gas. This nozzle has a length of 1m with a 19.1mm throat diameter, and a 211mm exit diameter, as illustrated in Fig. 1. When operated with carbon dioxide, this nozzle produced a reasonably uniform test core, but the nozzle exit Mach number was approximately 6. Pitot surveys indicated that there were no strong disturbances associated with the operation of this nozzle at the present off-design conditions.

Prior to a run, the nozzle, test section, and dump tank were evacuated to between 250 and 650Pa (the precise pressure does not influence the steady flow conditions within the nozzle core flow, but it does affect the transient nozzle flow starting process). The gun tunnel piston was made from Nylatron with an outer diameter of 96.3mm and a mass of 84grams.

A piezoelectric pressure transducer was positioned 153mm upstream of the nozzle entrance as illustrated in Fig. 1. The pressure history at this position is presented in Fig. 2. The result in Fig. 2 was actually formed by averaging the barrel pressure signal over the five runs used in the analysis of stagnation temperature results (Section 5.1).

The incident and reflected shock pressure levels illustrated in Fig. 2 are 1.10 ± 0.03 MPa and 4.45 ± 0.10 MPa respectively. The quoted uncertainty estimates arise because the indicated post shock pressure levels are not precisely steady. For each of the five gun tunnel runs, the mean barrel pressure within test time identified in Fig. 2 was within ± 0.10 MPa or $\pm 1.6\%$ of the five-run-average result, 6.36MPa. The barrel pressure transducer and associated charge amplifier were calibrated using a dead-weight tester. The

estimated uncertainty in the barrel pressure measurements is $\pm 1\%$.

3 Nozzle Exit Instrumentation

3.1 Stagnation Temperature Probe

A stagnation temperature probe consisting of platinum thin films located close to the stagnation point on the rounded tip of fused quartz rods (similar to that described in [13]) was positioned at the exit of the hypersonic nozzle, as illustrated in Fig. 1. Each of the fused quartz rods was 3mm in diameter, and the platinum films were less than 1mm in length. Thus, the films extended away from the nominal stagnation point of each probe a maximum angle of 10° . Previous results [15] indicate that at an angle of 10° from the stagnation point, the flow temperature at the boundary layer edge will be lower than the flow stagnation temperature by only 0.3% at hypersonic conditions. This means that the transient heat flux identified by the thin films can be accurately described by

$$q = h(T_0 - T_w) \quad (1)$$

where T_0 is within 0.3% of the flow stagnation temperature, T_w is the temperature of the probe as measured by the thin film, and h is the heat transfer coefficient for the thin film probe.

If the heat transfer coefficient for the film is known or can be approximated with reasonable accuracy, then it is possible to estimate the flow stagnation temperature directly using Eq. (1) with only one measurement of transient heat flux (and film temperature). Such an approach has been adopted in previous studies such as [6]. However, to estimate the heat transfer coefficient h , a knowledge of other flow parameters is necessary. In a hypersonic flow, the pitot pressure at the point of interest is sometimes the only parameter that is required to obtain a reasonable estimate of h . Values of pitot pressure that have been time-averaged over a period of around 1ms or longer can be obtained with relative ease and high accuracy (better than 2%) in many short-duration facilities. Thus, provided the flow is reasonably uniform or the distribution is known, time-averaged values of h can be obtained. However, estimating the magnitude of heat transfer coefficient fluctuations for frequencies greater than about 1kHz via measurements of pitot pressure at some other location can be difficult because of the spatial separation of the film and pitot pressure measurements and pitot probe bandwidth limitations.

For these reasons, the technique adopted in the present work involves the measurements of transient heat flux at different probe temperatures. Similar approaches have already been demonstrated in previous

studies [13],[14],[15],[16]. By adopting the multiple probe temperature approach, the need to identify the time-averaged or fluctuating heat transfer coefficient of the heat flux probes can be avoided. Instead, the heat transfer coefficient can actually be identified directly from the heat transfer and probe temperature measurements.

For the range of probe and flow stagnation temperatures considered in the present study, stagnation point boundary layer calculations indicate that the heat transfer coefficient is essentially independent of temperature. Thus, in principle, measurements at only 2 different film temperatures are required to identify both the flow stagnation temperature and the heat transfer coefficient. To minimize errors associated with the technique, the temperature difference between the films should be as large as possible, with one of the films operated as close as possible to the flow stagnation temperature. In the present application, a large temperature difference with one of the films operated at around 650K (matching the flow stagnation temperature) was most easily achieved using separate probes. However, because of the spatial separation, interpretation of the high frequency components of the heat flux typically requires measurements at additional thin film probe temperatures. For the present implementation of the stagnation temperature measurement concept, 3 thin film probes were operated at different initial temperatures for 5 nominally identical gun tunnel runs.

Prior to a gun tunnel run, the probes were positioned above the nozzle so that film 1 was adjacent to an electrical heater as illustrated in Fig. 1. Electrical heating power was applied for about 2 minutes prior to gun tunnel operation. During this time, there was a significant temperature rise at film 1. A temperature rise was also registered at film 2, and to a lesser degree at film 3. Immediately before the gun tunnel was fired, the probes were repositioned in approximately the centre of the nozzle – details of the actual position of each probe are given in Fig. 1.

The temperature-resistance characteristics of the films were identified through oven calibration over the full range of substrate operating temperatures. A calibration curve for each film was identified in the form

$$\frac{R - R_r}{R_r} = \alpha(T - T_r) + \beta(T - T_r)^2 \quad (2)$$

where the reference temperature was taken as $T_r = 20^\circ\text{C}$.

Figure 3 provides the temperature-resistance calibration data for film 2 and clearly demonstrates the significance of the quadratic term in Eq. (2). The broken line in Fig. 3 is a straight line based only on a water bath calibration which provided resistance data up to a maximum temperature of only 55°C . Unless the quadratic calibration term is included, the film temperature may be underestimated by around

50K at the higher operating temperatures.

3.2 Pitot Probe

Pitot pressure measurements were obtained at the nozzle exit using two different probe arrangements. The two pitot probes with 1.5mm diameter inlet tubes illustrated in Fig. 1 are representative of the preferred arrangement of pitot probes in the Oxford University Gun Tunnel. In this arrangement, a 2.5mm diameter piezoresistive pressure transducer is mounted within the housing about 15mm downstream of the probe tip. The pressure transducer is thereby offered a degree of protection against impacts from high speed particles that are occasionally present within the flow. Such arrangements are suitable for measurements up to frequencies on the order of 1kHz because of the acoustic resonance of the cavity ahead of the transducer.

To obtain pitot pressure data for comparison with the heat flux probe data, a second pitot probe arrangement was also utilized. This involved direct exposure of a 2.5mm diameter piezoresistive transducer to the Mach 6 carbon dioxide flow. A shock tube test on the pressure transducer indicated that its resonant frequency was around 430kHz which suggests accurate data might be obtained up to frequencies around 100kHz. The manufacturer's specifications indicate a flat frequency response up to 20kHz, but do not provide clear information on the response beyond this frequency. Results obtained with the 2.5mm diameter exposed pitot probe were filtered to provide fluctuation data at frequencies between 1 and 25kHz.

The location of the pitot probes and thin film probes relative to the hypersonic nozzle exit is illustrated in Fig. 1. Although the probes were in close proximity, and the inlets of the 1.5mm diameter pitot probes were 12mm downstream of the other probes, the Mach number of the flow and the offset of each probe was sufficient to ensure interference between the probes did not occur. This was confirmed with schlieren flow visualisation which indicated that the bow shock of each probe intersected the other probes well downstream of the sensitive stagnation region.

4 Temperature Probe Analysis

The transient heat flux at each level of pre-heating was identified from the measured surface temperature history using a finite difference routine that accounted for both the variable thermal properties of the quartz substrate and the hemispherical geometry of the probe tips [17]. Variable thermal properties of the quartz are important in the current application because the quartz probes can be heated to temperatures in excess of 600K and the surface temperature can rise more than 100K during the run, eg

Fig. 4. The hemispherical geometry of the probe tips is also significant because the total flow duration is around 60ms. Approximating the heat penetration distance as $4(\alpha t)^{1/2}$ ([19]), the heat penetrates to a depth of around 0.9mm or 60% of the probe radius. An approximate analytical solution of the transient conduction problem with curvature effects [18] could have been used, but it was more convenient to adopt the numerical approach as this also included the variable thermal properties. Examples of the measured probe surface temperatures and corresponding heat flux results are given in Fig. 4.

Transient thin film heat flux devices typically have a relatively high measurement bandwidth. Although it is possible to account for the thermal inertia of the thin film in a relatively simple manner [20], the usual approach is to treat the film as if it is in thermal equilibrium with the surface of the substrate on which it is mounted. The film thickness then limits the bandwidth to around 100kHz for platinum films painted on quartz substrates with an effective thickness of typically $0.35\mu\text{m}$, or 1.3MHz for vacuum deposited films with a typical thickness of $10\mu\text{m}$.

Voltages corresponding to the film temperature signals were digitised at a rate of 100kSamples/s for the numerical heat transfer analysis discussed above. These analogue voltages were also passed into a heat transfer analogue unit [21] that produced a voltage signal proportional to the transient heat flux for a one dimensional (flat plate) transient heat conduction process. Such signal conditioning is sometimes useful in transient heat transfer experiments because it avoids errors that can arise due the numerical manipulation of digitised temperature signals. The analogue voltages were converted into actual heat flux data for fluctuations at frequencies between 1 and 25kHz (for later comparison with pitot data that was available in this bandwidth) using a sensitivity that was a function of the probe surface temperature only. In effect, this higher frequency analysis neglects the probe curvature and spatial variations in thermal properties of the quartz due to temperature gradients within the substrate. However, this is appropriate because even at the lowest frequency (1kHz), the heat penetrates the quartz to less than 10% of the radius and the measured surface temperature fluctuations amount to less than 0.01K.

5 Results and Discussion

5.1 Gun Tunnel Stagnation Temperature History

Voltage signals corresponding to the various pressure and thin film measurements were acquired every $10\mu\text{s}$, a rate of 100kSamples/s. Post processing of the signals from the nominally identical gun tunnel runs included the temporal alignment of the time sequences from each run according to shock arrival times. A sequence of linear regressions was then identified at intervals of $10\mu\text{s}$ for the film temperature versus transient heat flux data from the nominally identical gun tunnel runs and the thin film probes

operated at different initial temperatures. According to Eq. (1), the slope of each linear regression within the sequence provides a measurement of h and the point on the regression line where $q = 0$ indicates the value of T_0 .

The stagnation temperature history identified by the sequence of linear regressions is presented in Fig. 5. The stagnation temperature history captures similar features to the stagnation pressure history (Fig. 2) including the initial shock compression process, although only the reflected waves are observed because the temperature probe is downstream of the barrel end. Another feature in evidence on both the stagnation pressure and the stagnation temperature records is the disturbance that arrives at the barrel end at approximately 40ms on the scale in Figs. 2 and 5.

To obtain an indication of the likely uncertainties associated with the linear regression analysis, two particular regressions are illustrated in Fig. 6. The slope of the lines in Fig. 6 is the inverse of the probe heat transfer coefficient, and the point on the regression line where $q = 0$ indicates the flow stagnation temperature. The data in Fig. 6a represents an average over the period 12ms to 14ms in Fig. 2, and the data in Fig. 6b represents an average over the period 57ms to 69ms corresponding the test time indicated in Fig. 2.

Figure 6b indicates that for two nominally identical gun tunnel runs, film 1 was pre-heated sufficiently to register a negative heat flux during the test time. However, within the reflected shock flow (Fig. 6a), film 1 was cooled by the test flow during only one of the two nominally identical gun tunnel runs in question. This situation arises because the flow stagnation temperature is not constant during the period of flow discharge from the nozzle. Figure 4 provides an illustration of this effect. Film 1 which had an initial temperature $T_{wi} = 618\text{K}$ (Fig. 4) was further heated by the flow during the first portion of the experiment (say $t < 20\text{ms}$ on the scale in Fig. 4), but in the latter portion of the experiment (around $t = 60\text{ms}$), the film was cooled by the flow. This is because the flow stagnation temperature falls with time (see Fig. 5), and reaches a temperature lower than that of film 1 during the test time.

An examination of Fig. 6 indicates a scatter in the data of around $\pm 10\text{K}$. A significant portion of this scatter may arise due to run-to-run variations in the initial temperature of the carbon dioxide within the barrel. A level of $\pm 2\text{K}$ was estimated for the uncertainty in the initial filling temperature (see Section 2) and this translates to around $\pm 4.5\text{K}$ after the compression process. Other factors that may contribute to the variability in the stagnation temperature include the barrel filling pressure, and the initial filling conditions of the air driver. In any case, run-to-run variations of around $\pm 10\text{K}$ for the present operating condition have been confirmed by an analysis of the run-to-run variations in the reflected shock wave's time-of-flight between the barrel pressure transducer, the piston, and back to the barrel pressure transducer.

Through close inspection of Fig. 6, it is possible to identify systematic differences between the results for each of the three films. Film 1 typically produces results very close to the regression, while film 2 results are slightly above, and 3 film results are slightly below the regressions illustrated in Fig. 6. The origin of these systematic errors has not yet been identified. However, the uncertainty in stagnation temperature measurement that arises from these systematic errors is estimated as around $\pm 10\text{K}$. Thus, these errors are not particularly significant in the present application because they are not greater than the run-to-run variations in stagnation temperature produced by the gun tunnel.

Following the piston deceleration and subsequent wave reflections between the piston and the end of the barrel (between approximately 15 and 20ms in Fig 5), the average stagnation temperature of the test gas decreases throughout the remainder of the flow. Spatial temperature gradients within the nozzle reservoir region may arise due to either the finite piston acceleration at the start of the compression stroke or turbulent heat transfer to the barrel during the compression stroke or during subsequent test gas discharge through the nozzle. As the piston accelerates to essentially its final velocity during the first metre of its nine metre stroke, the effects of finite piston acceleration are likely to be confined to about 10% of the test gas closest to the piston [1]. Since the stagnation temperature falls consistently throughout the duration of the flow, turbulent heat transfer from the test gas to the barrel appears the most probable cause of the temperature decay observed in Fig. 5.

The initial portion of the stagnation temperature history is reproduced in Fig. 7. This figure also includes the barrel (stagnation) pressure and nozzle exit pitot pressure signals for reference. The broken line in Fig. 7b indicates an estimate of the nozzle exit stagnation temperature for the reflected shock conditions based on the thermodynamic curves for CO_2 recommended by Reynolds [22], the initial CO_2 conditions within the barrel, and the pressure levels measured behind the incident and reflected shocks (see Fig 2). Following the initial flow establishment process between about 10 and 10.5ms on the scale in Fig. 7 there is excellent agreement between the temperature probe measurements and the predicted value up to about 11.5ms (the time indicated with the arrow in Fig. 7b).

The feature on the pitot signal that has been highlighted with the arrow, appears stronger for the gun tunnel runs with higher initial nozzle and test section pressures. (For the example given in Fig. 7, the initial pressure was approximately 650Pa.) As this feature on the pitot signal appears at about the same time as the drop in stagnation temperature (both features are indicated by the arrow in Fig. 7), it is thought that both are related to the nozzle flow starting processes. Comparison between measured and predicted reflected shock stagnation temperatures should be after a steady nozzle flow has been established (ie, for times after the arrow and up to approximately 15ms). The drop in stagnation temperature at the highlighted feature is approximately 10K, which is the same as the estimated run-to-run variability of the gun tunnel.

5.2 Fluctuation Measurements

An example of the fluctuations in pitot pressure (from the fast response 2.5mm diameter probe) and heat flux (from film 1) at the nozzle exit during the 12ms test time identified in Fig. 2 is presented in Fig. 8. During this 12ms period, the time-averaged pitot pressure over the 5 gun tunnel runs was $102\pm 2\text{kPa}$. The rms pitot pressure over the 5 gun tunnel runs was $0.56\pm 0.07\text{kPa}$.

At the start of the pitot pressure record presented in Fig. 8, the signal has a clear periodicity with a characteristic time of around 0.7ms. At this time (around 57ms on the scale in Fig. 2), the piston is passing over the barrel pressure transducer tapping, as is evidenced by the relatively low noise on the barrel pressure signal (examine Fig. 2 at the start of the indicated test time). This means the cavity length between the piston and the end of the barrel is around $l = 150\text{mm}$. During the test time, which is terminated by the complete drainage of carbon dioxide from the barrel, the average temperature within the remaining barrel test gas at approximately 57ms is estimated as 610K. This gives a speed of sound of $a = 375\text{m/s}$ and hence, unsteady acoustic waves which persist within the test gas following the shock compression and piston deceleration process are expected to have a period of about $2l/a = 0.8\text{ms}$, very close to the observed oscillation period of 0.7ms. It is therefore concluded that observed fluctuations in the nozzle exit pitot pressure arise largely because of reflected acoustic (isentropic) waves within the barrel test gas.

With isentropic fluctuations in the nozzle exit test gas properties, the fluctuations in stagnation temperature and pitot pressure will be related according to

$$\frac{T'_0}{T_0} = \frac{\gamma - 1}{\gamma} \frac{p'_{pit}}{p_{pit}} \quad (3)$$

where $\gamma = 1.21$ is the effective ratio of specific heats of the carbon dioxide test gas. The magnitude of the isentropic rms stagnation temperature fluctuations associated with the measured rms pitot pressure fluctuations of 0.55% will therefore be 0.58K.

Each quantity in Eq. (1) can be written in terms of time-averaged and fluctuating components, and then rearranged to give,

$$\frac{q'}{q} = \frac{h'}{h} + \frac{T'_0}{T_0 - T_w} - \frac{T'_w}{T_0 - T_w} + \frac{h'(T'_0 - T'_w)}{h(T_0 - T_w)}. \quad (4)$$

where the prime (') indicates fluctuations at frequencies between 1 and 25kHz, and all other symbols (without the prime) are now understood to indicate time-averaged values. For the present work, time-averaging was performed over the 12ms period corresponding to the test time indicated in Fig. 2.

For transient thin film heat flux gauges, the magnitude of fluctuations in surface temperature and heat flux are related in the frequency domain according to

$$\frac{|T'_w|}{|q'|} = \frac{1}{\sqrt{\omega}\sqrt{\rho ck}} \quad (5)$$

where ω is the angular frequency, and ρ , c , and k are the density, specific heat, and conductivity of the thin film substrate. Thus, for the present conditions where $h \approx 2.6\text{kW/m}^2\text{K}$ and $\sqrt{\rho ck} \approx 2000\text{J/m}^2\text{Ks}^{1/2}$ (at the elevated film temperatures), and the minimum frequency of interest is 1kHz, the largest anticipated fluctuation in thin film temperature can be expressed as,

$$\frac{|T'_w|}{T_0 - T_w} \approx 0.016 \frac{|q'|}{q} \quad (6)$$

Hence it is reasonable to neglect the second term on the RHS of Eq. (4) because it represents a contribution of less than 2%.

The last term in Eq. (4) is second order and is also neglected. Thus, to a good approximation, the fluctuations in the heat flux can be written as,

$$\frac{q'}{q} = \frac{h'}{h} + \frac{T'_0}{T_0 - T_w} \quad (7)$$

From Eq. (7) and Eq. (1) (in its time averaged form), it can be seen that when $T_w \approx T_0$, the fluctuations in heat flux are primarily due to stagnation temperature fluctuations and the two fluctuating quantities are related through the time-averaged heat transfer coefficient according to,

$$T'_0 = q'/h \quad (8)$$

The data presented in Fig. 8b is from a case where there was only a 10K difference between T_0 and T_w and indicates an rms fluctuation in heat flux of 6.8kW/m^2 . Time-averaged film temperature versus heat flux results during the test time (eg, Fig. 6b) gives an average heat transfer coefficient of $h = 2.56 \pm 0.15\text{kW/m}^2\text{K}$. Hence, the rms fluctuations in stagnation temperature estimated according to Eq. (8) would be around 2.7K.

Figure 9 illustrates the rms heat flux fluctuations obtained from the different probes over a range of $T_0 - T_w$ values. Figure 9 suggests that the actual value of q'_{rms} at $T_0 - T_w = 0$ is probably lower than 6.8kW/m^2 indicated by the data in Fig. 8b because some sensitivity to h' remains at $T_0 - T_w = 10\text{K}$ and

film 1 data systematically indicates larger values than film 2 (although film 1 data is roughly in agreement with film 3 data). Based on these considerations, q'_{rms} at $T_0 - T_w = 0$ is estimated as $6.0 \pm 0.8 \text{ kW/m}^2$, and hence rms stagnation temperature fluctuations are estimated as $2.3 \pm 0.3 \text{ K}$. As this value is significantly larger than the isentropic value of 0.58 K based on the pitot pressure measurements, it is concluded that entropy fluctuations are primarily responsible for the observed stagnation temperature fluctuations.

6 Practical Significance

The results demonstrate that the time-averaged stagnation temperature of the flow produced by the Oxford University Gun Tunnel can be identified with reasonable precision ($\pm 1.5\%$). The technique describe in this article should be considered by practitioners requiring a robust device that can produce high bandwidth stagnation temperature measurements over a short period of time (say less than 1sec).

Fluctuations in stagnation temperature have also been identified within the hypersonic flow produced by the Oxford University Gun Tunnel. The source of the stagnation temperature fluctuations is probably the turbulent heat transfer from the test gas to the barrel upstream of the hypersonic nozzle. Other gun tunnel and short-duration facilities with similar compression processes to that employed in the Oxford University Gun Tunnel are likely to produce similar fluctuations. Fluctuations in free stream properties may be significant in boundary layer transition experiments and other processes that are sensitive to free stream disturbances.

7 Conclusion

Implementation of a probe based on transient thin film heat flux gauges has allowed the identification of the stagnation temperature in a Mach 6 carbon dioxide flow produced by the Oxford University Gun Tunnel facility. The mean stagnation temperature at the hypersonic nozzle exit appears to fall at a reasonably steady rate throughout the duration of the flow. Turbulent heat transfer from the compressed test gas to the barrel is the most likely cause of the observed temperature decay.

Pitot pressure measurements at the nozzle exit indicate an rms level of 0.55% for frequencies between 1 and 25kHz. These pitot pressure fluctuations are related to acoustic fluctuations within the barrel test gas. Therefore, the observed pitot pressure fluctuations will be largely isentropic. The magnitude of the stagnation temperature fluctuations (again at frequencies between 1 and 25kHz) measured with the thin film probe (rms of 2.3 K) are significantly larger than the isentropic stagnation temperature fluctuations associated with acoustic fluctuations within the barrel test gas (rms of 0.58 K). Hence, it is concluded that

the stagnation temperature fluctuations at the exit of the hypersonic nozzle are largely attributable to entropy fluctuations. The source of the entropy fluctuations at the nozzle exit is probably the turbulent heat transfer from the compressed test gas to the barrel.

8 Future Research

Fluctuations in stagnation temperature have been identified at only one gun tunnel operating condition. It would be useful to clarify the relationship between the turbulent heat losses within the barrel and the stagnation temperature fluctuations at the nozzle exit. This could be achieved through additional experiments with flush-mounted transient heat flux gauges in the barrel. It would also be useful to perform sufficient parametric experiments to enable estimation of stagnation temperature or entropy fluctuations in other short-duration facilities.

Acknowledgement The authors wish to acknowledge the EPSRC for the provision of a Visiting Fellowship for DRB.

Nomenclature

a	speed of sound (m/s)
c	specific heat (J/kgK)
h	heat transfer coefficient at the thin film (W/m ² K)
k	conductivity (W/mK)
l	length of test gas slug remaining in barrel (m)
p	pressure (Pa)
p_0	stagnation pressure measured in the end of the barrel (MPa)
p_{pit}	pitot pressure measured at the nozzle exit (MPa)
q	heat flux (W/m ²)
R	thin film resistance (Ω)
R_r	thin film resistance at reference temperature (Ω)
T	temperature ($^{\circ}$ C or K)
T_w	probe surface temperature as indicated by the film (K)
T_{wi}	initial probe surface temperature just prior to flow establishment (K)
T_0	stagnation temperature measured at nozzle exit (K)
T_r	reference temperature in film calibration (20 $^{\circ}$ C)
t	time, arbitrary datum (ms)
α	linear coefficient in film calibration (K ⁻¹)
β	quadratic coefficient in film calibration (K ⁻²)
γ	ratio of specific heats (dimensionless)
ρ	density (kg/m ³)
ω	angular frequency (rad/s)
subscripts	
0	stagnation
r	reference
rms	root mean square value
superscripts	
'	fluctuating component

References

- [1] Cain, T.M., An Experimental Study of Under-Expanded Jets, D.Phil Thesis, Dept Eng. Sci., University of Oxford, 1992.
- [2] Shek, H.H-W.S., A Study of Moderately Underexpanded Single and Twinjet Rocket Exhaust Plumes in Quiescent and in a Mach 7 Hypersonic Freestream, Dept Eng. Sci., University of Oxford, 1997.

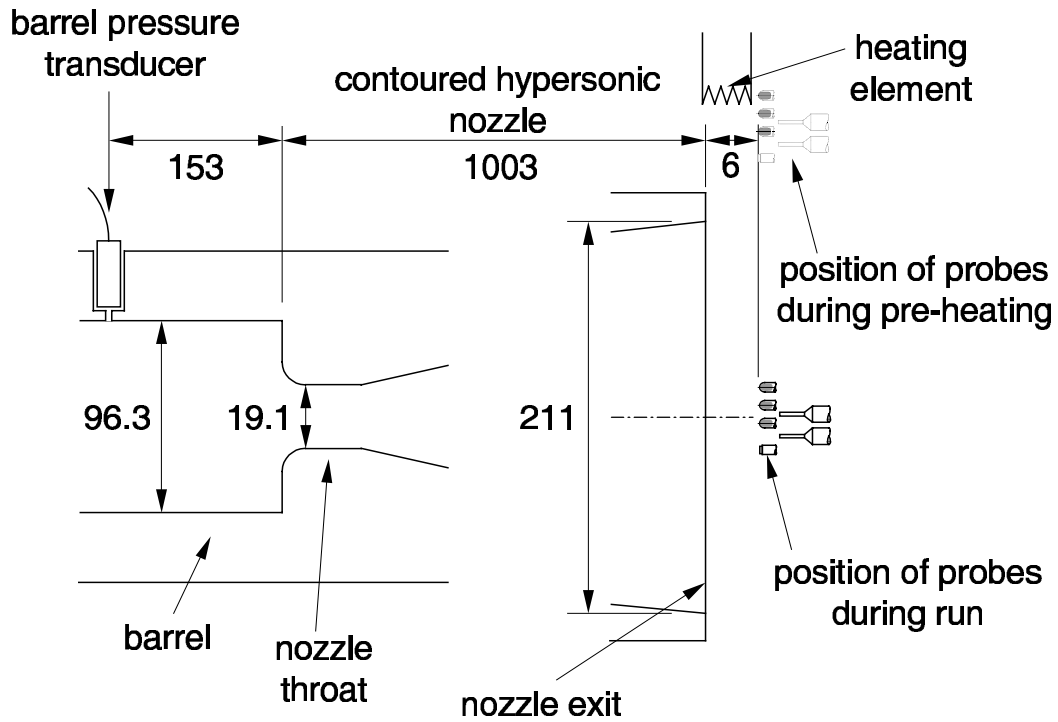
- [3] Buttsworth, D. R., Morgan, R. G., and Jones, T. V., Experiments on Oblique Shock Interactions with Planar Mixing Regions, *AIAA J.*, **35**(11), 1774-1777, 1997.
- [4] Buttsworth, D. R., Morgan, R. G. and Jones, T. V., A Gun Tunnel Investigation of Hypersonic Free Shear Layers in a Planar Duct, *J. Fluid Mech.*, **299**, 133-152, 1995.
- [5] Mallinson, S. G., and Hillier, R., Pressure Gradient Effects on Turbulent Hypersonic Boundary Layers, 21st International Symposium on Shock Waves, Paper 3740, Great Keppel, Australia, 1997.
- [6] Mallinson, S. G., Hillier, R., Jackson, A. P., Kirk, D. C., Soltani, S., and Zanchetta, M., Gun Tunnel Flow Calibration: Defining Input Conditions for Hypersonic Flow Computations, *Shock Waves*, **10**, 313-322, 2000.
- [7] Chen, F.-J., Wilkinson, S. P., and Beckwith, I. E., Gortler Instability and Hypersonic Quiet Nozzle Design, *J. Spacecraft and Rockets*, **30**(2), 170-175, 1993.
- [8] He, Y., and Morgan, R. G., Transition of compressible high enthalpy boundary layer flow over a flat plate, *Aeronautical J.*, **98**, 25-34, 1994.
- [9] Nagamatsu, H. T., Sheer, R. E. Jr., and Graber, B. C., Hypersonic Laminar Boundary-Layer Transition of 8-Foot-Long, 10° Cone, $M_1=9.1-16$, *AIAA J.*, **5**, 1245-1252, 1967.
- [10] Buttsworth, D. R., and Jacobs, P. A., Measurement of Fluctuations in a Mach 4 Shock Tunnel Nozzle Flow, 7th Australasian Heat and Mass Transfer Conference, pp. 53-59, Townsville, Australia, 2000.
- [11] Ng, W. F., and Epstein, A. H., High-Frequency Temperature and Pressure Probe for Unsteady Compressible Flows, *Rev. Sci. Instrum.*, **54**(12), 1678-1683, 1983.
- [12] Vas, I. E., Flowfield Measurements Using a Total Temperature Probe at Hypersonic Speeds, *AIAA J.*, **10**(3), 317-323, 1972.
- [13] Buttsworth, D. R., and Jones, T. V., A Fast-Response Total Temperature Probe for Unsteady Compressible Flows, *J. Eng. for Gas Turbines and Power*, **120**(4), 694-702, 1998.
- [14] Buttsworth, D. R., Jones, T. V. and Chana, K. S., Unsteady Total Temperature Measurements Downstream of a High Pressure Turbine, *J. Turbomachinery*, **120**(4), 760-767, 1998.
- [15] Buttsworth, D. R., and Jones, T. V., A Fast-Response High Spatial Resolution Total Temperature Probe using a Pulsed Heating Technique, *J. Turbomachinery*, **120**(3), 601-607, 1998.
- [16] Buttsworth, D. R., and Jacobs, P. A., Total Temperature Measurements in a Shock Tunnel Facility, 13th Australasian Fluid Mechanics Conference, Vol. 1, pp. 51-54, Melbourne, Australia, 1998.

- [17] Buttsworth, D. R., A Finite Difference Routine for the Solution of Transient One Dimensional Heat Conduction Problems with Curvature and Temperature-Dependent Thermal Properties, OUEL Report No. 2130/97, Dept Eng. Sci., University of Oxford, 1997.
- [18] Buttsworth, D. R., and Jones, T. V., Radial Conduction Effects in Transient Heat Transfer Experiments, *Aeronautical J.*, **101**(1005), 209-212, 1997.
- [19] Schultz, D. L., and Jones, T. V., Heat-Transfer Measurements in Short-Duration Hypersonic Facilities, AGARDograph No. 165, 1973.
- [20] Buttsworth, D. R., and Jones, T. V., Transient Thin Film Heat Flux Measurements with Finite Film Thickness, 21st International Symposium on Shock Waves, Paper 1661, Great Keppel, Australia, 1997.
- [21] Oldfield, M. L. G., Burd, H. J., and Doe, N. G., Design of Wide-Bandwidth Analogue Circuits for Heat Transfer Instrumentation in Transient Wind Tunnels, Proceedings 16th Symp. of International Centre for Heat and Mass Transfer, Hemisphere Publishing, pp. 233-257, 1982.
- [22] Reynolds, W.C., *Thermodynamic Properties in SI*, Department of Mechanical Engineering, Stanford University, 1979.

List of Figures

1	Illustration of the apparatus and instrumentation – dimensions in mm, not to scale. . . .	19
2	Stagnation pressure history measured within the barrel (5 run average).	20
3	Temperature-resistance calibration for film 2.	20
4	Examples of probe surface temperature and heat flux data.	21
5	Stagnation temperature history measured at the nozzle exit.	21
6	Probe surface temperature versus heat flux results for a number of nominally identical runs.	22
7	Initial shock processes and flow establishment in the gun tunnel.	22
8	Examples of fluctuations measured at the nozzle exit during the test time indicated in Fig. 2. a) pitot pressure fluctuations; b) heat flux fluctuations for $T_0 - T_w = 10\text{K}$	23
9	RMS heat flux fluctuations during the test time indicated in Fig. 2 for various probe surface temperatures approaching $T_0 - T_w = 0$	23

a) illustration of the barrel, nozzle, and probes



b) details of probe locations

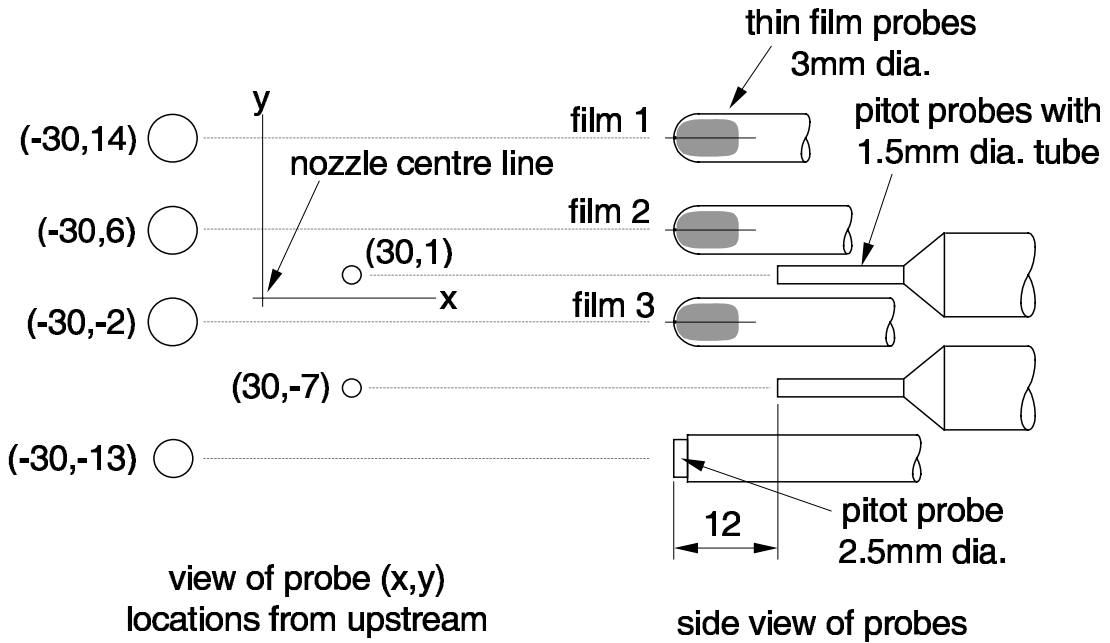


Figure 1: Illustration of the apparatus and instrumentation – dimensions in mm, not to scale.

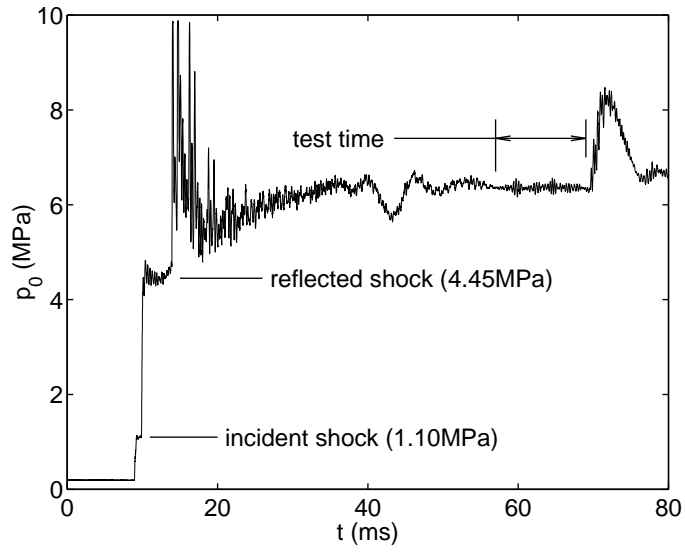


Figure 2: Stagnation pressure history measured within the barrel (5 run average).

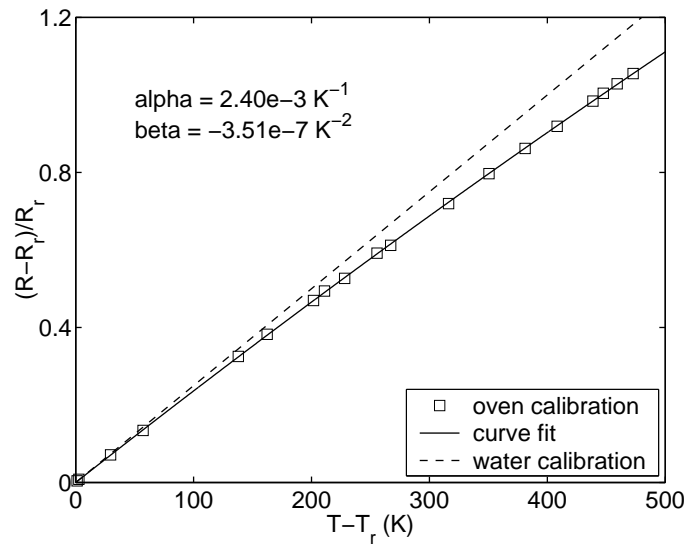


Figure 3: Temperature-resistance calibration for film 2.

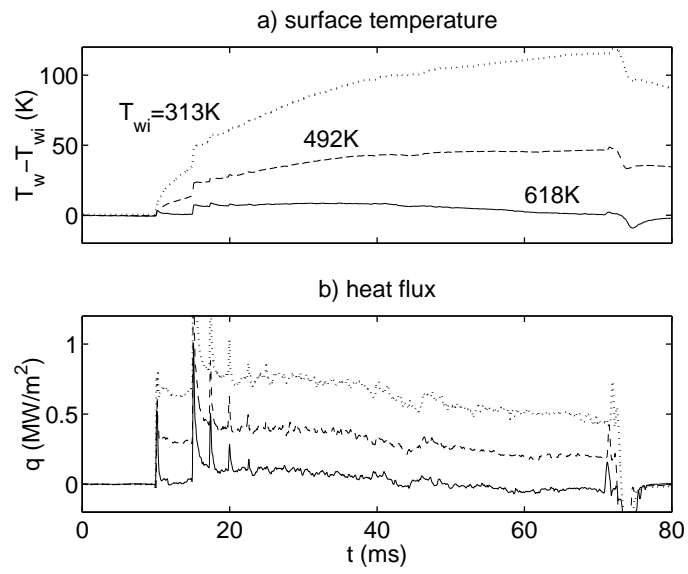


Figure 4: Examples of probe surface temperature and heat flux data.

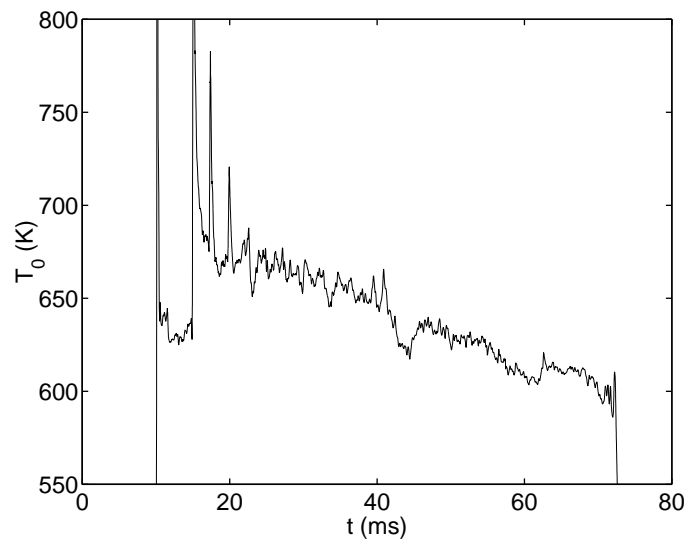


Figure 5: Stagnation temperature history measured at the nozzle exit.

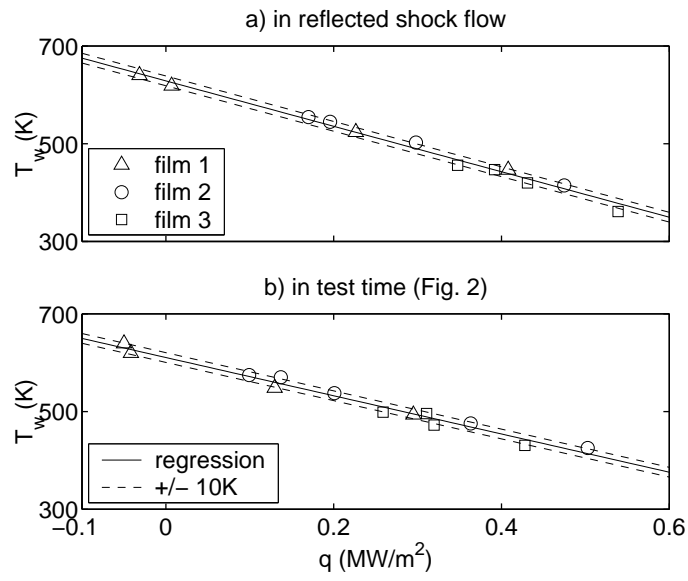


Figure 6: Probe surface temperature versus heat flux results for a number of nominally identical runs.

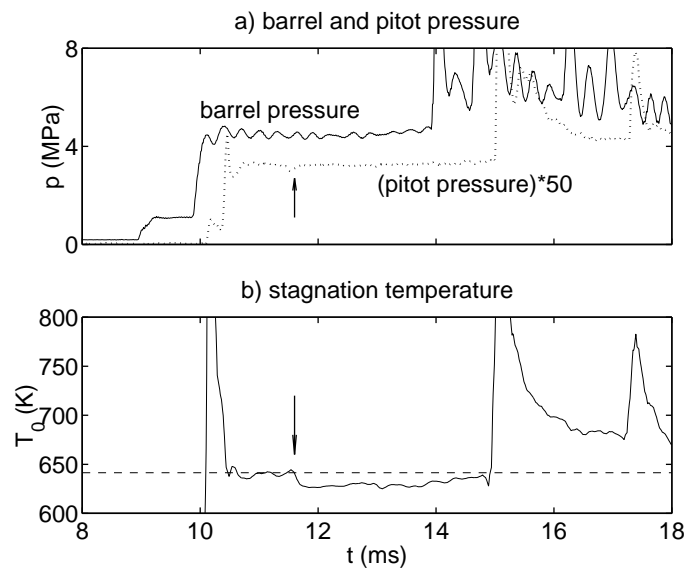


Figure 7: Initial shock processes and flow establishment in the gun tunnel.

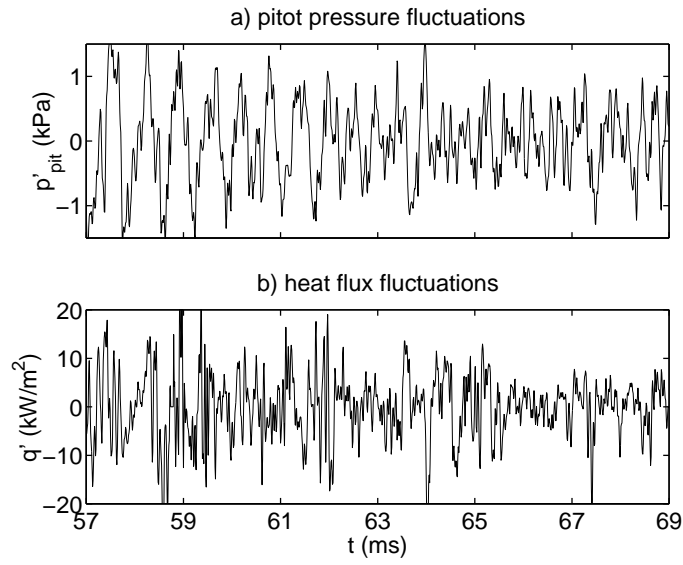


Figure 8: Examples of fluctuations measured at the nozzle exit during the test time indicated in Fig. 2. a) pitot pressure fluctuations; b) heat flux fluctuations for $T_0 - T_w = 10\text{K}$.

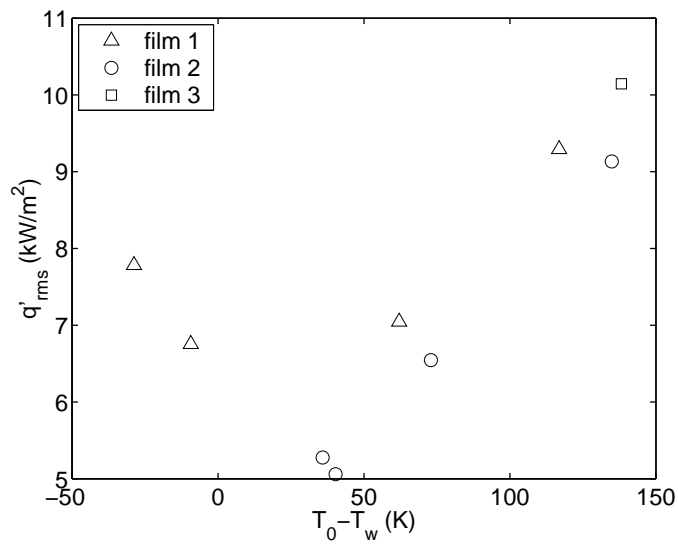


Figure 9: RMS heat flux fluctuations during the test time indicated in Fig. 2 for various probe surface temperatures approaching $T_0 - T_w = 0$.